Polymer 52 (2011) 258–265

Contents lists available at ScienceDirect

Polymer

journal homepage: www.elsevier.com/locate/polymer

Insight on the periodate oxidation of dextran and its structural vicissitudes

João Maia [a,*], Rui A. Carvalho [b,c], Jorge F.J. Coelho [a], Pedro N. Simões [a], M. Helena Gil [a]

[a] Chemical Engineering Department of the Faculty of Sciences and Technology of the University of Coimbra, Coimbra, Portugal
[b] Life Sciences Department of the Faculty of Sciences and Technology of the University of Coimbra, Coimbra, Portugal
[c] Center of Neurosciences and Cell Biology, Coimbra, Portugal

ARTICLE INFO

Article history:
Received 23 June 2010
Received in revised form
30 November 2010
Accepted 30 November 2010
Available online 8 December 2010

Keywords:
Oxidized dextran
Bidimensional NMR
Thermal analysis

ABSTRACT

Periodate oxidized dextran has been widely studied in a broad range of biotechnological applications, regardless of this, usually little attention is paid to the oxidation extension consequences on the properties of the final modified dextran. Based on a bidimensional NMR analysis, we suggest that the two aldehydes groups, resulting from the periodate oxidation, are not fully reactive with *N*-nucleophiles, under certain pH conditions. The aldehyde group bonded to C_3 appeared to be the only prone to react. The other aldehyde might be arrested in more stable hemiacetal structures. The hemiacetals are also responsible for oxidized dextran crosslinking, interfering in simple processing steps, such as dissolution and solubility, as well as increasing the viscosity of the solutions. The molecular weight variation on the oxidized samples can be followed by dynamic mechanical thermal analysis in consequence of the variation of glass transition temperature with the molecular weight, which was corroborated by the onset temperature of the thermal degradation.

1. Introduction

Dextran is a polysaccharide synthesized by a large number of bacteria, when grown on sucrose-containing media [1]. Nowadays, *Leuconostoc mesenteroids* (strain B-512) [2] is responsible for the majority of the commercially available dextrans. They are characterized by having over 95% of α-1,6 linkages and some low degree of branching. From the late 1940's, dextrans have attracted attention from the biotechnology world. They were accepted as a plasma volume expander, due to its linear structure, high water solubility, and especially owing to its α-1,6 linkage, more relevant to biological applications, in virtue of the slower hydrolysis by body enzymes, compared to the α-1,4 linkage (e.g. glycogen) [1,2].

The dextran oxidation by the periodate ion is a catalysis-free aqueous reaction which yields a purified product with a simple dialysis step. The periodate ion attacks vicinal diols promoting bond breaking. Typically, the α-1,6 residues in dextran are attacked between carbons C_3–C_4 or C_3–C_2, breaking the C–C bond and yielding aldehyde groups, being able to be further reduced on a second and independent oxidation reaction (Scheme 1) [3]. Initially, this method was used in the characterization and elucidation of the polysaccharide structure, through the complete oxidation and consequent analysis of the degradation products [4]. Nowadays, low and mild periodate oxidations are used to confer the dextran chain with aldehyde functionalities, which have as main characteristic the highly reactive nature towards *N*-nucleophiles, such as amines, hydrazines or carbazates [5].

Concerning the oxidized dextran (dexOx) application on a biomedical perspective, the accurate assessment of the periodate oxidation consequences in mild oxidation conditions is of utmost importance in predicting the extent of drug loading [6] or the final physico-chemical properties of hydrogels [7]. Due to the highly reactive nature of the formed aldehydes, they are easily attacked by neighbouring hydroxyl groups, leading to the formation of hemiacetals [8]. These hemiacetals are the most consensual resulting structures, even taking into account that some studies restrict these structures to a narrow pH window (4.0–5.2) [9]. Other consequences of the dextran oxidation are the decreased average molecular weight and polydispersity increase [10].

Herein we address the consequences of low and mild dextran oxidation and try to further elucidate the structural nature of dexOx through bidimensional NMR, upon reaction with *tert*-butyl carbazate. Our data suggest that only one aldehyde per residue might be involved on this reaction, while the second aldehyde could be arrested to a stable hemiacetal structure. We will explore the oxidation influence on simple manipulation steps, such as aqueous dissolution and the solutions viscosity outcome. Dynamic mechanical thermal analysis (DMTA) data on dexOx are discussed and correlated with the molecular weight trend. The relative thermal

* Corresponding author. Rua Sílvio Lima, Pólo II, Departamento de Engenharia Química, FCTUC, 3030-790 Coimbra, Portugal. Tel.: +351 239 798 743; fax: +351 239 798 703.
E-mail address: joaom@eq.uc.pt (J. Maia).

0032-3861/$ – see front matter © 2010 Elsevier Ltd. All rights reserved.
doi:10.1016/j.polymer.2010.11.058

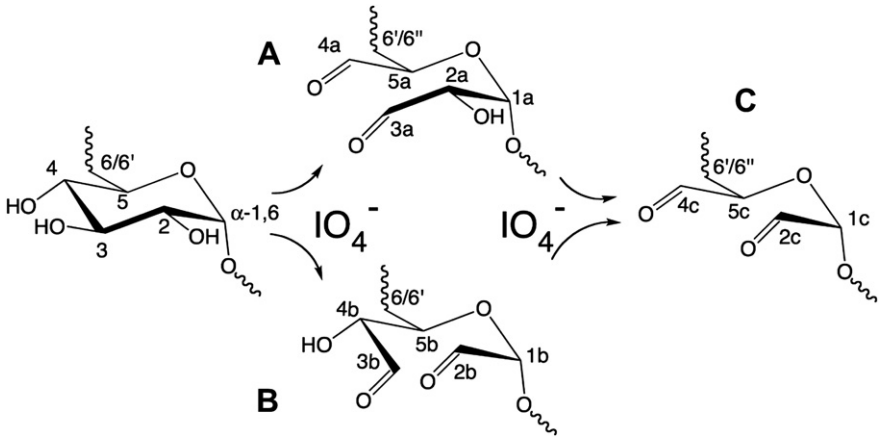

Scheme 1. Dextran's α-1,6 glucose residue possible periodate oxidations. (A) Periodate attack at C_3–C_4; (B) C_3–C_2 and (C) double oxidation.

stability of dexOx samples was evaluated by thermogravimetric (TG) measurements.

2. Materials and methods

2.1. Materials

Dextran (from Leuconostoc mesenteroides; M_w 60 kDa, according to Fluka's specification), sodium periodate, adipic acid dihydrazide (AAD), *tert*-butyl carbazate (tBC), ethyl carbazate (EtC), phosphate buffered saline (PBS; pH 7.4), dialysis membranes (MWCO 12 kDa) and NaOD were purchased from Sigma (Sintra, Portugal) and used as received.

2.2. Dextran oxidation

An aqueous solution of dextran (1 g; 12.5% (w/v) ~ pH 5.5) was oxidized with 2 mL of sodium periodate solution with different concentrations (33–264 mg/mL) to yield theoretical oxidations from 5 to 40%, at room temperature (The oxidation degree (OD) of dexOx is defined as the number of oxidized residues per 100 glucose residues). The reaction was stopped after 4 h. The resulting solution was dialyzed for 3 days against water and lyophilized (Snidjers Scientific type 2040, Tillburg, Holland). The scale-up of the reaction was done using the same procedure albeit using 30 g of dextran and a calculated amount of periodate to yield a theoretical oxidation of 5, 10, 25 and 40%, referred hereafter as D5, D10, D25 and D40, respectively.

2.3. Nuclear magnetic resonance (NMR)

^{1}H spectra were acquired on a Varian 600 NMR spectrometer (Palo Alto, CA) using a 3 mm indirect detection NMR probe with z-gradient. ^{1}H NMR spectra were recorded in D_2O (20–25 mg in 0.2 mL; pD of c.a. 4.5 or 10.2 after addition of NaOD) using a 90° pulse and a relaxation delay of 30 s. The water signal, used as reference line, was set at δ 4.75 ppm and was partially suppressed by irradiation during the relaxation delay. A total of 32 scans were acquired for each ^{1}H NMR spectra. Bidimensional spectra were recorded on the same magnet and probe. ^{1}H–^{1}H correlation spectroscopy (COSY) spectra were collected as a 2048 × 1024 matrix covering a 5 kHz sweep width using 32 scans/increment. Before Fourier transformation, the matrix was zero filled to 4096 × 4096 and standard sine-bell weighting functions were applied in both dimensions. ^{1}H–^{13}C heteronuclear multiple quantum coherence (HMQC) spectra were collected as a 2048 × 1024 matrix covering sweep widths of 5 and 25 kHz in the first and second dimensions, respectively. Before Fourier transformation, the matrix was zero filled to 4096 × 4096 and standard Gaussian weighting functions were applied in both dimensions. The spectra were analyzed with iNMR software, version 2.6.4 (www.inmr.net). The oxidation degree (OD) refers to the theoretical value unless otherwise stated.

2.4. DexOx's solubility and solutions viscosity

The different dexOx and dextran samples were dissolved in PBS (20% w/w). Aliquots of 1 mL were distributed in small glass vials, frozen at −20 °C and freeze-dried, in order to obtain a similar freeze-drying cake across every sample. The original dextran processed this way will be referred as D0. To each sample, 0.85 mL of miliQ water was added and the dissolution time was recorded at different temperatures ($n = 3$). The reason was to mimic the reconstitution of a pharmaceutical freeze-dried product. The vials were preserved under reduced pressure on a glass desiccator supplied with silica gel. Dextran and dexOx solutions, with concentrations ranging from 10 to 30% w/w, were prepared and tested in a Brookfield Programmable D-II$^+$ Viscometer with an S18 spindle, assisted by DVLoader v1.0 software. The chamber temperature was controlled by an external bath to 25 °C. Low viscosity solutions were measured by a Labolan V1-R viscometer with an LCP spindle (low viscosity adapter) and controlled temperature to 25 °C.

2.5. Size exclusion chromatography

Performed in an HPLC system composed by a degasser and a WellChrom Maxi-Star k-1000 pump (Knauer), coupled to an LS detector (evaporative light scattering PL-EMD 960) and one column (Polymer Laboratories, aquagel-OH Mixed 8 μm). The whole system was kept at room temperature and the eluent used was KNO_3 (0.001 M; pH 3.9) at a flow rate of 0.4 mL/min. Samples and standards were dissolved in the eluent at 4–6 mg/mL (Fluka Chemie AG, dextran standards from 12 to 80 kDa).

2.6. Dynamic mechanical thermal analysis

The freeze-drying samples obtained above were subjected to dynamical mechanical thermal analysis (DMTA) on a Triton Tritec 2000 analyzer. About 50 mg of sample were loaded into metal pockets fabricated from a sheet of stainless steel. The pocket was clamped directly into the DMTA using a single cantilever configuration. Temperature scans, from −200 °C to +300 °C with a standard heating rate of 2 °C min^{-1} were performed in

a multifrequency mode (1 and 10 Hz) in order to identify the temperature transition peaks.

2.7. Thermogravimetric analysis

The thermal stability of dextran and dexOx samples was studied in a TA Instruments Q500 thermogravimetric analyzer (thermobalance sensitivity 0.1 μg). The temperature calibration was performed in the range 25–1000 °C by measuring the Curie point of nickel standard, using open platinum crucibles, a dry nitrogen purge flow of 100 mL min^{-1}, and a heating rate of 10 °C min^{-1}, the later being the conditions applied throughout the thermoanalytical measurements. At least two runs were performed for each sample (sample weights of ca. 8 mg) in order to check the repeatability of measurements.

3. Results and discussion

3.1. DexOx characterization

Dextran with a molecular weight of 60 kDa, was oxidized with variable amounts of sodium periodate in order to obtain different

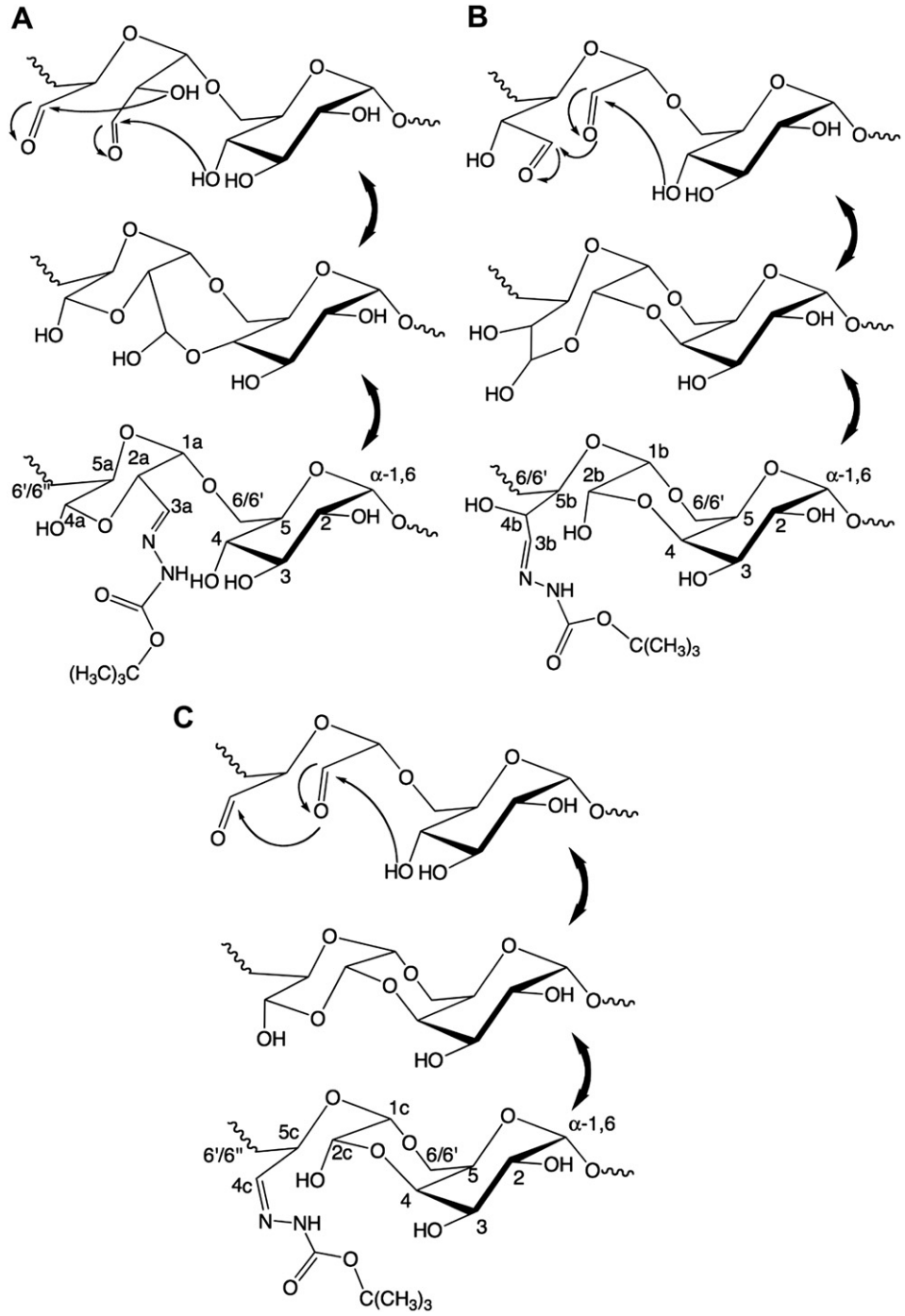

Scheme 2. (A) Single periodate oxidation outcome after periodate ion attack at C_3–C_4 and (B) C_3–C_2 cleavage, followed by possible intra-hemiacetals formation and tBC reaction. (C) Periodate doubly oxidized residue, possible hemiacetals and tBC reactions.

OD. Usually, the aldehyde group is not observed by FTIR spectroscopy, unless in highly oxidized samples (1730 cm^{-1}), nor in the NMR spectrum, except during the first minutes of reaction (~9.7 ppm) [10]. It is widely accepted that the aldehyde groups react with nearby hydroxyl groups, forming hemiacetals or hemialdals [3,8]. These transitory events could be either intra or inter-residue (Scheme 2) and, in certain situations, interfere with the oxidation evolution. The most important aspect arising from this modification is the final oxidation degree. It defines the dexOx's reactivity on drug conjugation[6]or gelation rate on hydrogel formulations [7,10]. Concerning the estimation of the oxidation degree, several ways have been used to approach the problem. On extensive oxidations, acid-base titration is useful in assessing the released formic acid and the percentage of doubly oxidized residues [4].

On mild oxidations, colorimetric titrations, such as the hydroxylamine hydrochloride[11]or the TNBS assay [12], have been

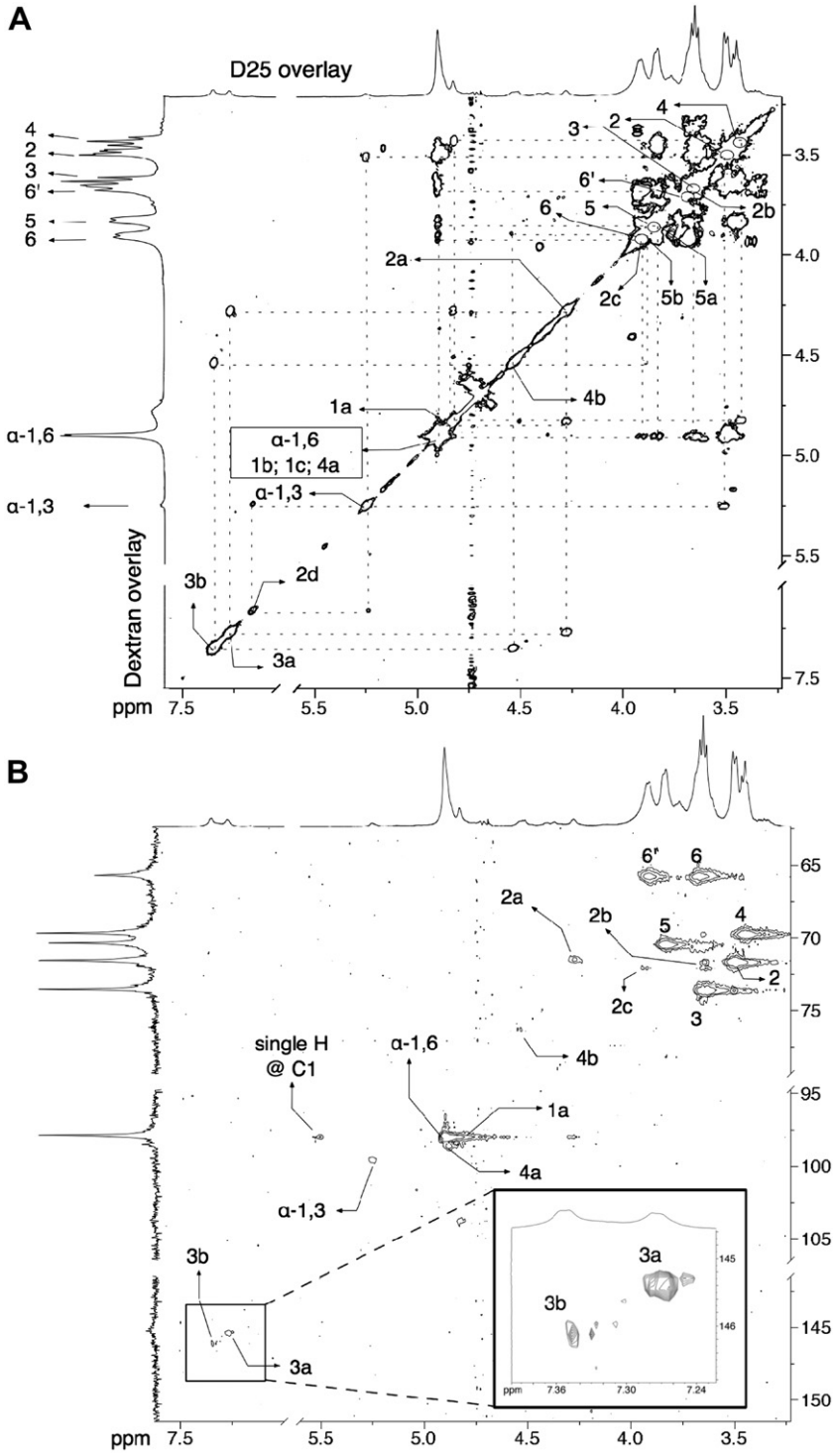

Fig. 1. (A) COSY and (B) HMQC spectra of D25. The peaks assigned with plain numbers refer to correlations arising from the intact residue. The correlations arising from the different oxidized residues are represented by: a: C_3–C_4 oxidation; b: C_3–C_2 oxidation; c: C_4–C_2 double oxidation; and d: α-1,3 branched oxidized residue.

used. However, the calculations are usually performed assuming that both aldehydes react with the carbazates. On an earlier study [10], our two-dimensional NMR results led us to suggest that just one of the aldehydes per residue reacts with the carbazates, in agreement with the single correlation observed on the $^{1}H-^{13}C$–HMQC spectrum. Our new results suggest that, under the studied conditions, only one aldehyde per residue is reacting.

3.2. Bidimensional NMR

The NMR data was collected in D_2O with a measured pH of ~4.5, which falls inside the consensual pH window for hemiacetals formation. Therefore, our bidimensional NMR analysis will take into account the most likely hemiacetal populations, based on previously proposed structures found in the literature. These structures will serve as a starting ground for the carbazone peak assignment. The C_3-C_4 cleavage (Scheme 1A) was described to be 7.5-fold faster than the C_3-C_2 cleavage (Scheme 1B) [8]. On a mild oxidation, the double oxidized structure (Scheme 1C) is likely less representative, as most periodate would be rapidly consumed on single oxidations and such scenario is favored by the starting pH (~5) [13]. Furthermore, it is thought that the hemiacetal formation could hinder further oxidation, even of neighboring residues [8]. Therefore, the structures arising from the C_3-C_4 oxidation will be treated as more representative, followed by the C_3-C_2 oxidation and the double oxidation. The titration of dexOx with carbazates yields a carbazone moiety, evidencing the former aldehydic proton, which helps clarifying the bidimensional spectra. The region around 7.3 ppm (proton axis) and 145 ppm (carbon axis) on the $^{1}H-^{13}C$–HMQC (Fig. 1B inset) unveiled two main peak populations of carbazone protons. A third carbazone peak exists (7.16 ppm), only seen on the COSY (correlation spectroscopy) spectrum (Fig. 1A) and is apparently correlated with the α-1,3 anomeric proton (see left axis dextran's proton spectrum overlay for the native peaks). Therefore, it seems to exist two main carbazone peaks, out of four possible different carbazones (C_2, C_4 and two different C_3's), though each of them could have different environments influencing the chemical shifts. Analyzing the C_3-C_4 cleavage (Scheme 2A), an intra-hemiacetal structure is likely to occur, after a hydroxyl (C_2) attack to the C_4 aldehyde, forming a stable six sides ring [14], despite several different possibilities due to the rotativity of the oxidized residue. The aldehyde on C_3 could suffer an attack from any hydroxyl group (HO–C_4 from the downstream residue suggested in the structure). We propose that this aldehyde would be the more susceptible of attack by tBC, represented by the most shielded of the protons (Fig. 1A 3a; ~7.28 ppm) in the 7.3 ppm region. Analyzing this peak correlation on the COSY, one can see a correlation with a proton at ~4.25 ppm (2a), correlating itself with a carbon (Fig. 1A) on the same chemical shift as glucose C_2 (~71.6 ppm). The same proton (2a) further correlates downfield, with a possible anomeric proton/carbon (1a). Considering this structure as the most likely and stable after C_3-C_4 cleavage, frames the C_4 proton in an anomeric-like environment and possibly could be associated with a correlation with C_5 like those proposed according to the bidimensional spectra (4a and 5a, respectively).

The C_3-C_2 cleavage yields an aldehyde on C_2, which has been proposed to form a stable and conformationally plausible 1,4-dioxepane ring after reaction with the OH on C_4 from the downstream residue (Scheme 2B) [8]. Again, the aldehyde on C_3 (3b) would be more prone to react with tBC. Following the other carbazone proton at ~7.35 ppm (Fig. 2B; 3b), it correlates with a proton at ~ 4.55 ppm (4b), which further correlates with a single proton upfield, falling near the glucose residue proton/carbon 5 (5b). There is a strong correlation between an anomeric proton and a proton at ~3.65 ppm, which could be an unshielded proton on C_2 and also

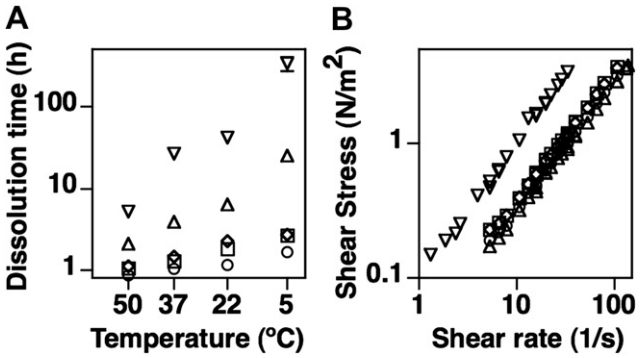

Fig. 2. (A) Dissolution time profiles, at different temperatures and (B) the shear stress vs. shear rate profile at 20% (w/w) concentration and 25 °C for dextran (○), D5 (□), D10 (◇), D25 (△) and D40 (▽).

correlates with a carbon in the same chemical shift as glucose C_2. This correlation could likely arise from 1b to 2b, but also 1c and 2c, from the doubly oxidized residue, being the environments very similar. Regarding the doubly oxidized residue, the hemiacetal structure depicted in Scheme 2C was also suggested by Ishak and Painter (1978) [8] to be plausible. Therefore, C_4 would be more sensitive to a carbazate attack. However, the third major visible correlation in the COSY spectrum, at 7.16 ppm, apparently correlates with the anomeric proton (α-1,3), which would be an unlikely chemical shift for a proton on C_5. It would be more reasonable if this correlation arose from the carbazate attack at C_2 of the doubly oxidized, but a second correlation would have to be present in the HMQC spectrum (Fig. 1B). It is possible that the correlations from the doubly oxidized residue, as well as other minor populations, are masked within the major peaks. The transient nature of the hemiacetals and the similar environments turn the peak assigning task a hard mission, which could have several interpretations. Anyhow, the two main correlations on the COSY spectrum suggest that not every aldehyde is reacting with a carbazate under these pH conditions.

At alkaline pH (10.2), some new peaks can be seen in the range of 7.5–9.5 ppm for the D25 sample (Supplementary Fig. 1A). These peaks were previously attributed to isomeric enol forms. Such structures are under an aldo–enol equilibrium [15]. Many other peak populations are observed between 4 and 6 ppm, due to the higher resolution (Supplementary Fig. 1A). Though, the addition of EtC, at this pH, did not revert most of the identified new peaks, it presented more correlations on the zone of interest for the carbazone protons (~7.3 ppm; Supplementary Fig. 1B and C). We have observed before, that dexOx crosslinked with AAD hydrogels dissolved quickly at pH 9 [10], suggesting the sensitivity of the hydrazone bond to alkaline pH's, thus, the likelyhood of a similar behavior for the carbazone bond also exists. These new correlations, suggest that, every aldehydic carbon is sensitive to a carbazate attack. Under this pH, the aldo–enolic structures are likely more exposed to attack than under the hemiacetal form, establishing a higher number of equilibriums, concomitantly expressed on the COSY spectrum (Supplementary Fig. 1D). The overlay of both COSY spectra shows the appearance of a high number of new correlations after the addition of EtC (Supplementary Fig. 1D, black contour), partially reverting the correlations of D25 (red contour). These results identify pH as a strong modulator of dexOx reactivity, which might be interesting to contemplate under certain pH sensitive applications.

3.3. Macroscopic consequences of the oxidation

The extensive and complete dextran oxidation leads to the destruction of the molecule into characteristic degradation by-

products [4]. Low and mild oxidations also degrade dextran, leading to slight molecular weight decrease. The destruction of the glucose residue, yielding aldehydes, could also contribute in altering the dexOx behavior in solution. The periodate oxidation in non-buffered solutions leads to pH decrease, after formic acid release [10], possibly contributing for acid-hydrolysis [16]. This phenomenon can be observed in several ways. The reference technique in the characterization of polymers is the size exclusion chromatography (SEC), which separates the different populations in accordance with the hydrodynamic volume, which can be translated to molecular weight and the polydispersity index (Table 1). The molecular weight is a key property of polymers, defining certain macroscopic characteristics, such as solubility, viscosity and clearance rates in biological systems [17]. Besides ^{1}H NMR and SEC, we have gathered results of techniques and empirical evidences, which clearly reflect the molecular weight differences between the several dexOx samples. One direct consequence of the dextran oxidation is the longer dissolution times in aqueous media. This phenomenon is of utmost importance on an off-the-shelf freeze-dried product. The dissolution time periods of the several samples under exactly the same conditions (Fig. 2A) but at different temperatures show that D5 and D10 have very close dissolution profiles to dextran (D0). However, the D25 and D40 dissolution profiles clearly reflect the OD increase. The viscosity of a dextran solution is directly related to the increment of concentration and M_w [18,19]. The molecular weight decreasing, due to periodate oxidation, should theoretically yield a less viscous solution than the original dextran, for the same concentration conditions. At lower concentrations (5%) the viscosity variation is negligible (Table 1). However, the reactivity of the oxidized dextran, through inter-hemiacetals formation, has great influence on the behavior of the solutions. We observed that the oxidation degree could invert the viscosity trend, depending on the dexOx concentration. Concentrated solutions favor the inter-chain hemiacetals formation, resembling a molecular weight increasing, hence the higher resistance to flow. Within the same concentration range (20% w/w), only D25 viscosity falls below the dextran viscosity. On the other hand, D40 has an extremely high resistance to flow, reflecting the cross-reactivity (Table 1 and Fig. 2B). We suggest that this effect is due to the inter-chain hemiacetals formed, inverting what would be the natural viscosity trend and demonstrating how both parameters (OD and M_w) can interfere with the viscosity of a given dexOx solution.

Table 1
Macroscopic characteristics of native dextran and the several oxidized samples. OD estimated by ^{1}H NMR analysis, M_w and PDI calculated by SEC, viscosities at different concentrations and time necessary until complete dissolution.

Sample	Oxidation degree		M_w[c]	PDI[d]	η[e] 20%	η[f] 5%	$t_{37\,°C}$[g] (hours)
	IO_4^-[a]	EtC[b]	kDa		(m Pa s)	(m Pa s)	
Dextran	–	–	60.1	1.47	30.7	2.7	1.0 ± 0.04
D5	5	3.6 ± 0.1	61.2	1.59	35.9	2.9	1.3 ± 0.08
D10	10	8.6 ± 0.2	60.8	1.61	35.1	3.0	1.5 ± 0.05
D25	25	22.2 ± 0.7	60.3	2.03	26.8	2.7	3.9 ± 0.65
D40	40	33.0 ± 0.8	25.4	3.05	102.8	2.7	26.6 ± 0.44

[a] Theoretical OD, calculated as the molar ratio of sodium periodate per initial glucose unit in dextran.
[b] Calculated by ^{1}H NMR after titration with ethyl carbazate, taking into account the ratio between the integral of the peak at δ 7.3 ppm and the integral of the anomeric proton at δ 4.9 ppm. Five independent integrations.
[c] Weight–average molecular weight estimated by SEC.
[d] Polydispersity index corresponding to M_w/M_n.
[e] Viscosities of dextran and oxidized dextrans at 20% w/w. Taken from the slope of the curves Shear Stress = f(Shear Rate) plot. The linear regression was forced to cross the origin as every sample showed a Newtonian behavior.
[f] Viscosities of dextran and oxidized dextrans at 5% w/w, at 200 rpm.
[g] Dissolution time taken, at 37 °C, in PBS, without agitation.

3.4. Thermal analysis

We have extended the study on the influence of the oxidation extension by analyzing the thermoanalytical curves of the different oxidized species. DMTA methods is frequently used to evaluate the effects of excipients on polymer's glass transition temperature (T_g). In amorphous polymers, a primary relaxation transition may be observed at the characteristic temperature T_g. In this point, the glass-like state (restricted motion of the polymeric chains) changes to a rubber-like state indicating loss in rigidity (*i.e.* increased relaxation) associated with enhanced polymeric chain mobility. Typically, the glass transition is defined as the temperature(s) at which either a maximum in the mechanical damping parameter (tan δ) or loss modulus (G″) occurs [20]. The presence of moisture can also be assessed by DMTA, being visible in the thermoanalytical curves as characteristic transitions at certain temperatures [21]. In terms of damping, it is possible to identify four main transitions for the original dextran, approximately at −80 °C, 105 °C, 235 °C and 305 °C (Fig. 3A*/**). The peak at −80 °C is a secondary relaxation due to absorbed water, which contributes to the formation of a more diffuse and stronger H-bond network than observed in a dry sample [21]. The peak at 105 °C refers to the water evaporation from dextran. These thermal events show that even after the freeze-drying process some residual water is present. These events have different profiles on the oxidized samples (not shown), which will not be addressed since this issue is out of the scope of this work. The next peak at ca. 235 °C corresponds to T_g (**). At this temperature, the storage modulus decreases rapidly and is frequency dependent on the Tan δ (Fig. 3A inset). This peak reflects an α-relaxation from non-frequency dependent events, such as crystallization, melting, curing or thermal degradation [22]. The peak at 305 °C reflects an overall degradation stage and will be discussed further ahead.

It has been reported that the molecular weight of dextrans influences the T_g due to the decrease of the free volume with the M_w increase [23]. To confirm such influence, the thermoanalytical data of several dextrans (M_w: 580, 60 and 19.5 kDa; tested as supplied) were analyzed. In fact, the T_g of the tested dextran samples decrease directly with the M_w, being the correspondent peak values observed at 237.8, 235.4 and 231.1 °C, respectively (Fig. 3B). These T_g values are in agreement with the trend described by Icoz et al. [23]. For a comparable M_w range, despite determined by a different technique. The different oxidized samples were processed in a similar way to avoid any artifacts that could arise from freezing and freeze-drying and there was an effort to minimize the samples moisture.

Interestingly, D0 presented a broader peak and shifted to lower temperature (223.6 °C) when compared with the original dextran (Fig. 3B). The presence of the phosphate salts could interfere with the freezing process of dextran, leading to different dextran chain conformation, which is reflected by the broader T_g peak and the shift to lower temperatures [24]. By freeze-drying a phosphate buffered aqueous dextran solution, it can impair the crystallization process of the salts [25] as well as the dextran derivative itself. Nevertheless, the M_w difference, within the dexOx's samples, is clearly visible on the DMTA curves (Fig. 3C and Table 2) corroborating the SEC and NMR data. It is known that crosslinking agents can also increase the T_g [20]. However, the hemiacetals crosslinking effect, observed on the viscosity studies, apparently is not reflected on the T_g, suggesting that the real molecular weight is dominant on the T_g onset.

A first look to the TG curve profiles (Fig. 4A) allows to identify a quite dramatic change in going from native dextran to its processed (freeze-dried PBS solution) counterpart, D0. Apart from a shift in the onset temperature of the main mass loss stage towards lower temperatures (by 41 °C), a remarkable difference is observed in the residual mass (at 600 °C), which should be ascribed to the

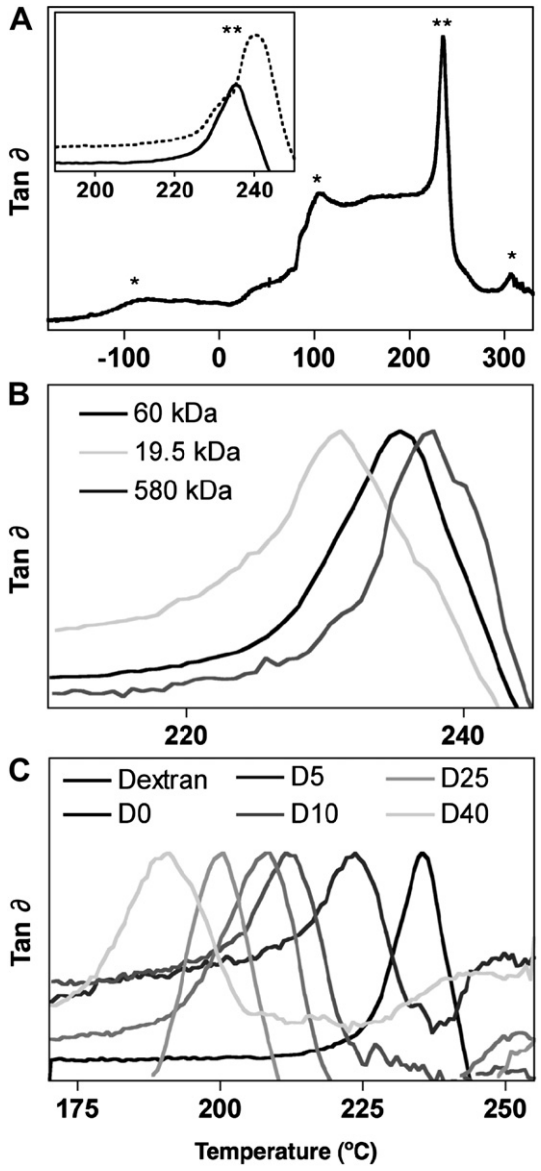

Fig. 3. (A) Full thermogram of native dextran marked with the non-frequency dependent transitions (*) and T_g identification through frequency dependent transition (** and inset); (B) T_g of the different molecular weight dextrans; (C) T_g of the different oxidized samples. All samples presented with a frequency of 1 Hz, except for dotted line at a frequency of 10 Hz.

salts coming from PBS. The original dextran exhibits a quite familiar behavior [21,26–28], with a first mass loss stage below ca. 120 °C due to the elimination of water, as observed in the DMTA, followed by the overall degradation stage (depolymerization) along the approximate temperature range from 298 to 328 °C, in good correspondence with the fourth transition, identified by the DMTA results (Fig. 3A). However, the thermal decomposition of oxidized dextran samples should be analyzed with reference to thermal decomposition of the sample that reflects the influence of PBS in dextran, D0. In this case, the differences in the thermoanalytical curves appear to be more subtle.

Both D0 and oxidized dextran samples exhibit a first mass loss stage, from the ambient temperature to 150 °C. The correspondent mass loss rate is somewhat variable among the samples, but the residual mass at 150 °C is quite comparable (see Table 2). This first weight change is caused by the loss of adsorbed water, and, probably, of some water of crystallization related with the PBS

Table 2
Glass transition temperatures obtained from the DMTA curves and characteristic quantities (mean and standard deviation) obtained from the TG/DTG curves.

Sample	T_g (°C)	T_{on}[a] (°C)		T_p[b] (°C)	Δm[c] (%)	
Dextran	235.5	298.6 ± 0.4		315.0 ± 0.2	92.8 ± 0.2	8.3 ± 0.4
D0	223.6	257.6 ± 1.4		269.9 ± 1.7	96.3 ± 1.1	29.7 ± 0.2
D5	211.5	195.2 ± 1.4	247.5 ± 0.8	267.1 ± 1.6	94.7 ± 0.2	29.7 ± 0.2
D10	207.9	198.6 ± 0.6	241.5 ± 0.4	279.2 ± 0.2	93.2 ± 0.3	28.8 ± 0.0
D25	200.5	190.8 ± 0.4	234.1 ± 0.3	266.2 ± 0.2	93.1 ± 0.4	30.9 ± 0.3
D40	190.7	179.7 ± 0.2	233.0 ± 0.7	274.4 ± 1.8	94.3 ± 0.3	35.4 ± 0.0

[a] T_{on}: extrapolated onset temperatures (TG curve).
[b] T_p: peak temperature, corresponding to the maximum decomposition rate (DTG curve).
[c] Δm: residual mass at the temperatures 150 °C and 600 °C.

components (phosphates). Above 150 °C, the differences in the response of samples under comparison become more apparent. The complexity of the global thermal decomposition, probably involving several kinetically independent processes as suggested by the TG data and, mainly, by the differential thermogravimetric (DTG) curves profiles (Fig. 4B), increases with the degree of the oxidation of the samples. A first change in the mass loss rate within the approximate temperature range 180–220 °C can be observed (Fig. 4B inset), being only incipient in the case of the D5 sample, moderate in the D10 one, and rather evident in the remaining oxidized dextran samples (see also Table 2 for the onset temperatures). This stage is followed by the main decomposition process, whose pattern is also clearly influenced by the oxidation degree, as revealed by the DTG curve profiles. In terms of characteristic quantities, while the onset temperature of the main decomposition stage obeys to a well defined pattern, monotonically decreasing with the increase of the oxidation degree from 247.5 °C (D5) to 233.0 °C (D40), the undefined trend of the peak temperature at the maximum decomposition rate (Table 2) reflects differences in

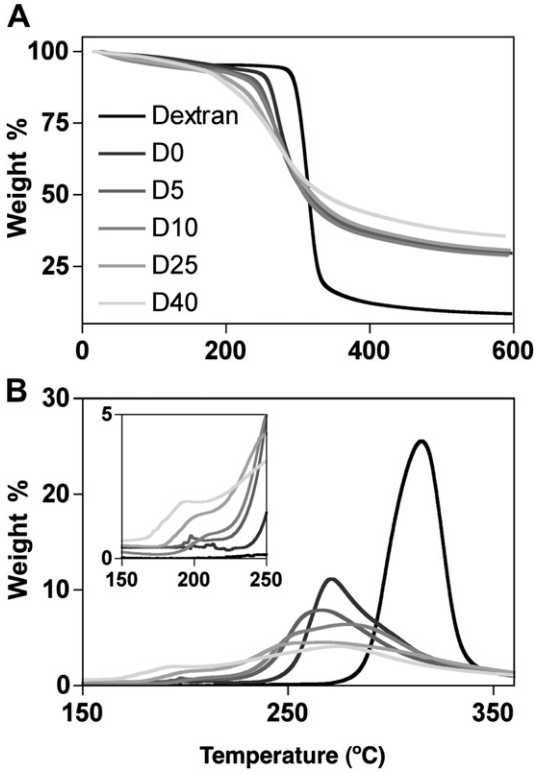

Fig. 4. (A) TG and (B) DTG curves of dextran and dexOx samples. ($\Phi = 10$ °C min^{-1}; dry nitrogen at 100 mL min^{-1}).

decomposition pathways. The residual mass at 600 °C for the most oxidized sample (D40) suggests a pronounced different decomposition course when compared to the remaining oxidized samples.

4. Conclusions

Our bidimensional NMR data suggests that only one aldehyde per residue is responding to the carbazate under mildly acidic conditions. We propose that the two main peak populations (~7.3 ppm) arise from carbazates on C_3 from single oxidized residues. There are more downfield shifted peaks, but not more than 5.5 ppm, which indicate the non-existence of more carbazate proton populations. These peaks should arise from protons involved in hemiacetals, which form anomeric-like environments. At alkaline pH, the aldehyde groups appear to be under different structures than hemiacetals. The enol forms appear to be more reactive towards carbazates, though more labile and less stable.

The periodate oxidation of dextran is a harsh reaction which promotes chain degradation, confers high chemical reactivity to a natively neutral molecule and deeply alters its physico-chemical properties. The increasing OD, impairs water solubility, taking longer periods of time to solubilize, and interferes with the resulting viscosity, especially at high polymer concentrations. The solutions viscosity could impair injectability and mixibility of certain formulations.

The degree of oxidation is also reflected on the glass transition temperature according to DMTA data. Interestingly, the hemiacetals do not seem to affect the thermal properties of the freeze-dried samples. The glass transition temperatures shift is in direct accordance with the molecular weight decrease, but do not give much insight on the structural consequences of the oxidation. On the other hand, the DTG profiles, for the diverse samples, are quite interesting. An increase in the thermal decomposition complexity with the increase in the oxidation degree was identified, evidencing the deleterious effect of periodate oxidation on dextran's structure. Low oxidative conditions, up to 10%, do not damage extensively dextran's structure, however milder oxidation conditions, result in extensive disruption of the dextran structure. These set of results may rise awareness for the consequences of periodate oxidation on the final structural properties of the modified dextran, helping researchers to better guide the design of dexOx-based formulations.

Acknowledgements

The authors thank Carla Ventura for the support on the viscosity studies. JM acknowledges the finantial support of Instituto de Investigação Interdisciplinar (III/BIO/20/2005).

Appendix. Supplementary data

Supplementary data related to this article can be found online at doi:10.1016/j.polymer.2010.11.058.

References

[1] Sidebotham RL. Adv Carbohydr Chem Biochem 1974;30:371–444.
[2] Bixler GH, Hines GE, McGhee RM, Shurter RA. Ind Eng Chem 1953;45:692–705.
[3] Guthrie R. Adv Carbohydr Chem 1961;16:105.
[4] Jeanes A, Wilham C. J Am Chem Soc 1950;72:2655–7.
[5] Suvorova OB, Iozep AA, Passet BV. Rus J App Chem 2001;74:1016–20.
[6] Hudson S, Langer R, Fink GR, Kohane DS. Biomaterials; 2009.
[7] Maia J, Ribeiro MP, Ventura C, Carvalho RA, Correia IJ, Gil MH. Acta Biomat 2009;5:1948–55.
[8] Ishak MF, Painter TJ. Carbohydr Res 1978;64:189–97.
[9] Drobchenko SN, Isaevalvanova LS, Kleiner AR, Lomakin AV, Kolker AR, Noskin VA. Carbohydr Res 1993;241:189–99.
[10] Maia J, Ferreira LS, Carvalho R, Ramos MA, Gil MH. Polymer 2005;46:9604–14.
[11] Zhao H, Heindel ND. Pharm Res 1991;8:400–2.
[12] Bouhadir KH, Hausman DS, Mooney DJ. Polymer 1999;40:3575–84.
[13] Novikova EV, Tishchenko EV, Iozep AA, Passet BV. Rus J App Chem 2002;75:985–8.
[14] Aalmo KM, Grasdalen H, Painter TJ, Krane J. Carbohydr Res 1981;91:1–11.
[15] Drobchenko SN, Isaevalvanova LS, Kleiner AR, Eneyskaya EV. Carbohydr Res 1996;280:171–6.
[16] Basedow AM, Ebert KH, Ederer HJ. Macromolecules; 1978.
[17] Mehvar R. J Control Rel 2000;69:1–25.
[18] Ioan CE, Aberle T, Burchard W. Macromolecules 2000;33:5730–9.
[19] Xu X, Li H, Zhang Z, Qi X. J App Polym Sci 2009;111:1523–9.
[20] Jones DS. Int J Pharm 1999;179:167–78.
[21] Scandola M, Ceccorulli G, Pizzoli M. Int J Biol Macromol 1991;13:254–60.
[22] Coelho JFJ, Carreira M, Goncalves PMOF, Popov AV, Gil MH. J Vinyl Addit Tech 2006;12:156–65.
[23] Icoz DZ, Moraru CI, Kokini JL. Carbohydr Polym 2005;62:120–9.
[24] Izutsu K, Heller MC, Randolph TW, Carpenter JF. J Chem Soc Far Trans 1998;94:411–7.
[25] Randolph TW. J Phamaceutical Sci 1997;86:1198–203.
[26] Hussain MA, Shahwar D, Tahir MN, Sher M, Hassan MN, Afzal Z. J Serb Chem Soc 2010;75:165–73.
[27] Katsikas L, Jeremic K, Jovanovic S, Velickovic J, Popovic I. J Therm Anal 1993;40:511–7.
[28] Tang M, Dou H, Sun K. Polymer 2006;47:728–34.